Genetically Encoded Calcium Indicators for In Situ Functional Studies of Corneal Nerves

Matthew T. McPheeters,[1] Brecken J. Blackburn,[1] William J. Dupps Jr.,[1–3] Andrew M. Rollins,[1] and Michael W. Jenkins[1,4]

[1]Department of Biomedical Engineering, Case Western Reserve University, Cleveland, Ohio, United States
[2]Cole Eye Institute, Cleveland Clinic Foundation, Cleveland, Ohio, United States
[3]Department of Biomedical Engineering, Lerner Research Institute, Cleveland Clinic, Cleveland, Ohio, United States
[4]Department of Pediatrics, Case Western Reserve University, Cleveland, Ohio, United States

Correspondence: Michael Jenkins, 2109 Adelbert Rd., Wood Building Rm WG28, Cleveland, OH 44106, USA;
mwj5@case.edu.

Received: July 7, 2020
Accepted: September 28, 2020
Published: November 5, 2020

Citation: McPheeters MT, Blackburn BJ, Dupps WJ Jr., Rollins AM, Jenkins MW. Genetically encoded calcium indicators for in situ functional studies of corneal nerves. *Invest Ophthalmol Vis Sci.* 2020;61(13):10. https://doi.org/10.1167/iovs.61.13.10

Purpose. Millions of people suffer from diseases that involve corneal nerve dysfunction, caused by various conditions, including dry eye syndrome, neurotrophic keratopathy, diabetes, herpes simplex, glaucoma, and Alzheimer's disease. The morphology of corneal nerves has been studied extensively. However, corneal nerve function has only been studied in a limited fashion owing to a lack of tools. Here, we present a new system for studying corneal nerve function.

Methods. Optical imaging was performed on the cornea of excised murine globes taken from a model animal expressing a genetically encoded calcium indicator, GCaMP6f, to record calcium transients. A custom perfusion and imaging chamber for ex vivo murine globes was designed to maintain and stabilize the cornea, while allowing the introduction of chemical stimulation during imaging.

Results. Imaging of calcium signals in the ex vivo murine cornea was demonstrated. Strong calcium signals with minimal photobleaching were observed in experiments lasting up to 10 minutes. Concentrated potassium and lidocaine solutions both modulated corneal nerve activity. Similar responses were observed in the same neurons across multiple chemical stimulations, suggesting the feasibility of using chemical stimulations to test the response of the corneal nerves.

Conclusions. Our studies suggest that this tool will be of great use for studying functional changes to corneal nerves in response to disease and ocular procedures. This process will enable preclinical testing of new ocular procedures to minimize damage to corneal innervation and therapies for diminished neural function.

Keywords: corneal nerves, functional imaging, calcium imaging, genetically encoded calcium indicators

The cornea is the outermost tissue of the anterior eye and critical to vision. The cornea and tear film are maintained by the corneal nerves, whose peripheral sensory terminals are densely integrated into the corneal epithelium.[1,2] Numerous diseases, such as diabetes mellitus, herpes simplex, glaucoma, and Alzheimer's disease, detrimentally affect the ocular surface, likely through deleterious effects on the function of the corneal nerves.[1,3–10] Diseases such as dry eye syndrome and neurotrophic keratopathy, which are principally of the ocular surface, are at least partially due to abnormal corneal nerve function.[11–16] Additionally, common ocular procedures such as refractive surgery and corneal cross-linking cause damage to the corneal nerves and can result in long-term morbidities.[2,17–21] These conditions and diseases collectively affect millions of people in the United States and many more worldwide.[22–27]

Study of the corneal nerves has been conducted in human subjects for a number of years using confocal microscopy to image nerve morphology and aesthesiometers to broadly assess sensitivity and function.[6,28–30] From that work, it is known that the corneal nerves change in response to disease, surgery, and aging.[31] There is significant interest in treatments to improve the condition of the corneal nerves in disease, as evidenced by the development and recent approval by the U.S. Food and Drug Administration of recombinant human nerve growth factor (Oxervate, Dompe, Milan, Italy)[32] to treat neurotrophic keratopathy. However, the limited range of tools for studying corneal innervation has made it difficult to assess the progression of corneal neuropathy and the efficacy of treatments. Understanding how corneal nerve signaling changes during normal development and during disease progression, such as in type 1 diabetes, may provide insight into the etiology of eye diseases and neurologic disorders. Before progress on understanding the role of corneal nerve function in disease states can be made, better tools need to be developed and refined. Such tools would enable development of new treatments for corneal nerve dysfunction.

Previous functional study of corneal nerves has been limited by a lack of experimental techniques.

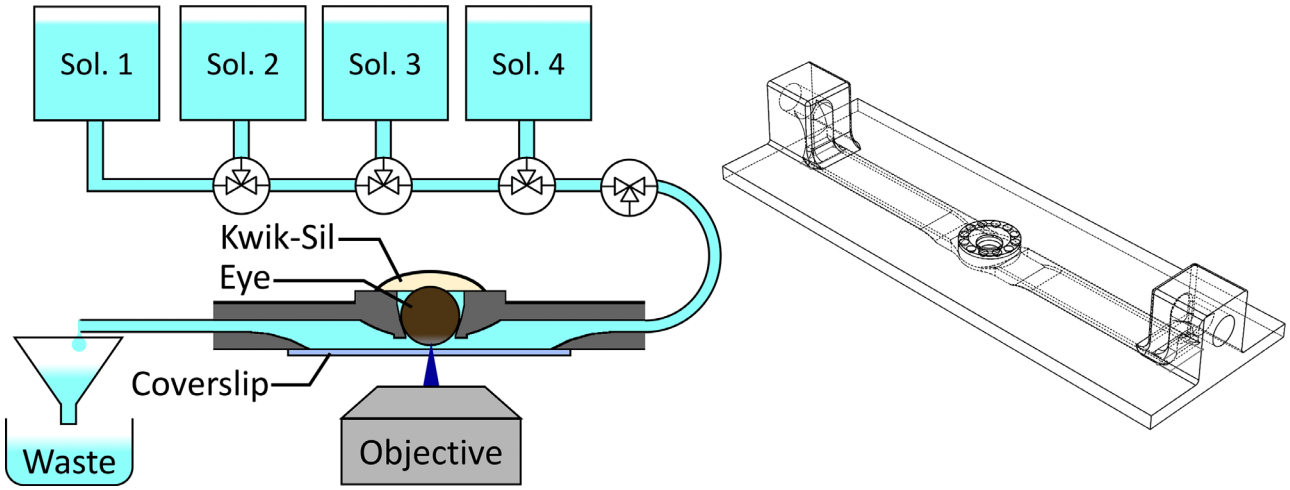

Figure 1. A schematic of the continuous flow apparatus and sample chamber designed to allow stable imaging of the ex vivo globe. A murine globe is suspended above a cover slip in a microscope-slide (25 × 75 mm) sized chamber, designed to allow solutions to be continuously flowed past the cornea while imaging. The cornea is held in place by a low-toxicity silicone adhesive, such as Kwik-Sil. An arbitrary number of reservoirs and a manifold can be used to control which solution flowed past the cornea, and a break pressure chamber was used after the imaging chamber to minimize motion owing to suction from gravitational forces on the fluid in the outflow line.

Electrophysiologic methods have been used both on the ciliary nerves of excised globes and directly on the corneal surface.[33,34] Direct measurement of the ciliary nerves has informed much of what is known about the function of the corneal nerves. Additionally, fluorescent calcium reporter dyes, which change in fluorescence in response to changes in calcium concentration, have been used to image cultured or excised corneal neurons.[35–37] Although this is a promising approach, the use of calcium dyes requires detergents to get into the corneal neurons and tend to be at least somewhat phototoxic. Most recently, genetically encoded calcium indicators (GECIs) have been used to image excised and cultured nerves.[38] While this work is promising, further development of tools for functional study in situ and in vivo is needed to study the long term effect of injury and disease on the corneal nerves.

Here, we introduce an experimental model and preparation that allows for functional imaging of the corneal innervation in an ex vivo murine globe. The overarching goal of this work is to develop tools to study functional changes to the corneal nerves. This approach may enable a better understanding of the mechanisms of ocular surface homeostasis in health and disease, which ultimately may be used to develop treatments, optimize procedures, and minimize injury to the ocular surface.

Methods

Mouse Strains

All animal work was performed in adherence with the ARVO Statement for the Use of Animals in Ophthalmic and Vision Research. GECIs for high-fidelity Ca^{2+} imaging in excitable cells are used to study neural circuitry in the brain and peripheral nervous system. When paired with the appropriate promoter, murine models express GECIs in specific neural subtypes or in all neurons. For use in the cornea, we crossed a C57BL mouse strain with a plasma membrane-targeted GCaMP6f conditional allele (Jackson stock #029626) to a C57BL mouse strain expressing nestin cre (JAX stock #003771).[39,40] The nestin cre was chosen because it is a promoter for a type VI intermediate filament prominent in nerve cells.[40,41] The model only needs to be heterozygous for both the GCaMP6f conditional allele and the nestin cre to achieve expression of GcaMP6f. This model strongly expresses GCaMP6f in the corneal nerves, observed as a strong blue/green fluorescent signal (Fig. 1). Several other transgenic murine lines with GCaMP6f expressed against other promoters (including VGLUT2, Chat, and Thy1) were also tested and found not to strongly express GCaMP6f in the corneal nerves. We found that we achieved the best results with animals at least 3 months old because expression of GCaMP6f in the corneal nerves was observed to gradually increase after birth.

Tissue Preparation

All animal experiments were performed according to protocols (Jenkins 2016-0042, 2019-0015) approved by the Institutional Animal Care and Use Committee of Case Western Reserve University. Mice were sacrificed by isoflurane overdose followed by cervical dislocation. Both globes were enucleated, taking care to preserve as much of the ciliary nerves as possible, and placed in artificial cerebral spinal fluid (aCSF) (124 mM NaCl, 2.7 mM KCl, 1.25 mM $NaH2PO_4$, 10 mM $MgSO_4$, 3 mM $CaCl_2$, 26 mM $NaHCO_3$, 18.6 mM dextrose, and 2 mM ascorbic acid; pH = 7.3–7.4). Globes were then immediately used for imaging or chilled on ice. Although it is known that the corneal nerves begin to degenerate quickly postmortem,[42] we found that chilled globes were observed to still display basal nerve signaling visible with functional imaging after being returned to room temperature at least 3 hours postmortem. An example of this is shown in Supplementary Figure S3. Each experiment shown results from the testing of a single globe.

Imaging

All imaging was done using a Leica SP8 confocal microscope. The microscope was inverted and a 10×/0.4 NA air

Investigative Ophthalmology & Visual Science

objective (Leica HC PL APO CS 10×/0.40 DRY) was used. The 488-nm line of an argon ion laser was used for excitation in our experiments with a typical average power of 165 µW. Light in the 500-580nm range was collected by the SP8 hybrid detector. A custom sample chamber was designed to minimize globe motion while imaging (model included in the Supplementary Data). In the chamber, the globe is suspended just above a #0 coverslip (EMS 63750-01) without applanating the cornea. A low-toxicity silicone adhesive (Kwik-Sil, WPI, Sarasota, FL) was placed over the back of the globe to help hold it in place and prevent dehydration. The 2.5-mm diameter opening in the chamber is expected to expose most or all of the mouse cornea (2.3- to 2.6-mm diameter[43]) to fluid flow. We observed in early experiments that addition of buffers and chemicals to the sample chamber would cause the globe to move. To address this phenomenon, we designed a continuous flow apparatus in which buffer is continuously passed around the cornea while imaging. The solution can easily be changed to introduce drugs or other chemicals to the solution without altering the fluid force on the cornea. Depending on how well the globe is mounted, sometimes there is a small motion artifact when changing between solutions owing to the fluid flow change from opening or closing a valve. Most of the time, the image remains highly stable both axially and laterally during imaging. A schematic of our imaging chamber and setup is shown in Figure 1. The use of a break pressure chamber (shown as a funnel in Fig. 1) after the imaging chamber was critical to eliminating both unwanted suction and motion owing to the dripping of fluid after exiting the imaging chamber.

Chemical Stimulus

Various chemical stimuli were applied to the cornea to stimulate or inhibit neural activity. aCSF was used as the storage solution and buffer. 0.3 M KCl (Thermo Fisher Scientific, Waltham, MA) and 10 mM lidocaine (Sigma-Aldrich) were added to aCSF for stimulation or inhibition and the solutions were checked and adjusted as necessary to ensure a pH of 7.3-7.4.

Image Processing

Data processing, analysis and image visualization were done using Matlab 2019b (Mathworks, Natick, MA), ImageJ, Fiji, Amira 6 (Thermo Fisher Scientific, St Louis, MO) and Photoshop 21 (Adobe, San Jose, CA).[44,45] A piecewise rigid motion correction algorithm for calcium imaging data (NoRMCorre) was used for image registration.[46] All plots of data show fluorescence amplitude in time without baseline correction to demonstrate rate of photobleaching. The signal-to-noise ratio (SNR) was quantified as the peak height above baseline over the standard deviation of the baseline in regions without apparent action potentials. The $\Delta F/F_0$ was quantified as the difference between peak height and the averaged baseline in regions without apparent action potential divided by the baseline.

Results

We assessed the expression of GCaMP6f in the cornea by recording a scanned volume of a globe excised from an adult transgenic mouse and placed in aCSF. Axial and lateral projections of this three-dimensional image are shown in Figure 2. Many of the corneal nerves are clearly visible and traceable from the ciliary nerve bundles to the sensory nerve terminals which project into the corneal epithelium. This matches the expected structure of the corneal nerves, depicted in Supplementary Figure S1 and described in the literature.[47]

To assess the functional response of our reporter in the cornea, we prepared an ex vivo globe as described and imaged baseline activity at room temperature with buffer flowing past the cornea as shown in Figure 1. The results are shown in Figure 3 and Supplementary Video S1. Strong calcium transients corresponding prefer to action potentials were observed. Approximately 165 µW of average

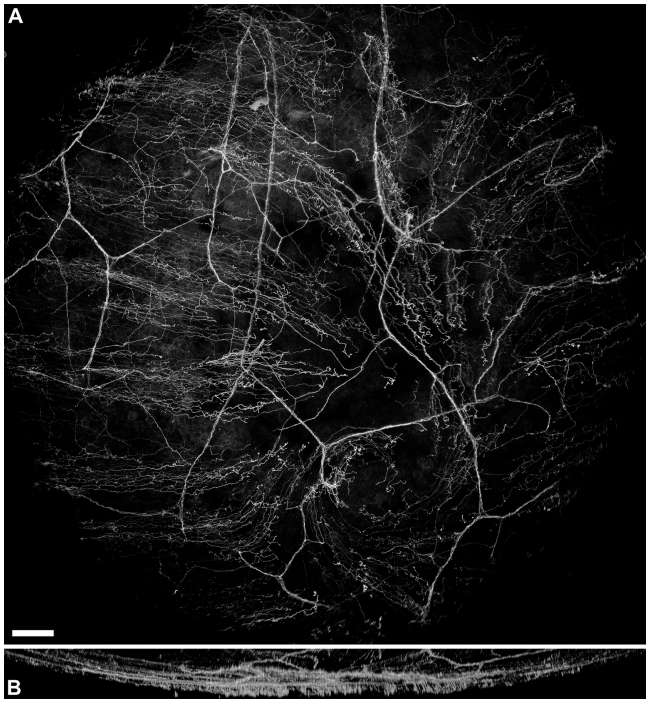

Figure 2. (**a**) Axial intensity projection of a murine cornea expressing GCaMP6f against the nestin promoter. Scale bar is 100 µm. (**b**) Lateral intensity projection of the middle half of the dataset shown in (**a**). GCaMP6f is broadly expressed and appears to be visible across all of the layers of the cornea, from the stroma to sensory nerve terminals in the corneal epithelium.

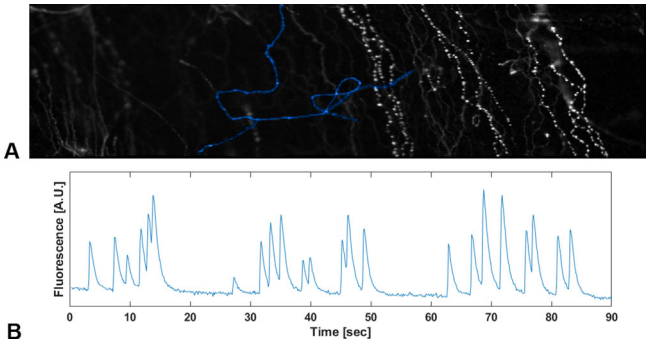

Figure 3. (**a**) Average intensity projection of a region of murine cornea with a region of interest (ROI) highlighted in blue. The scale bar is 100 µm. (**b**) The fluorescent trace for the ROI shown in (**a**) over a period of 90 seconds.

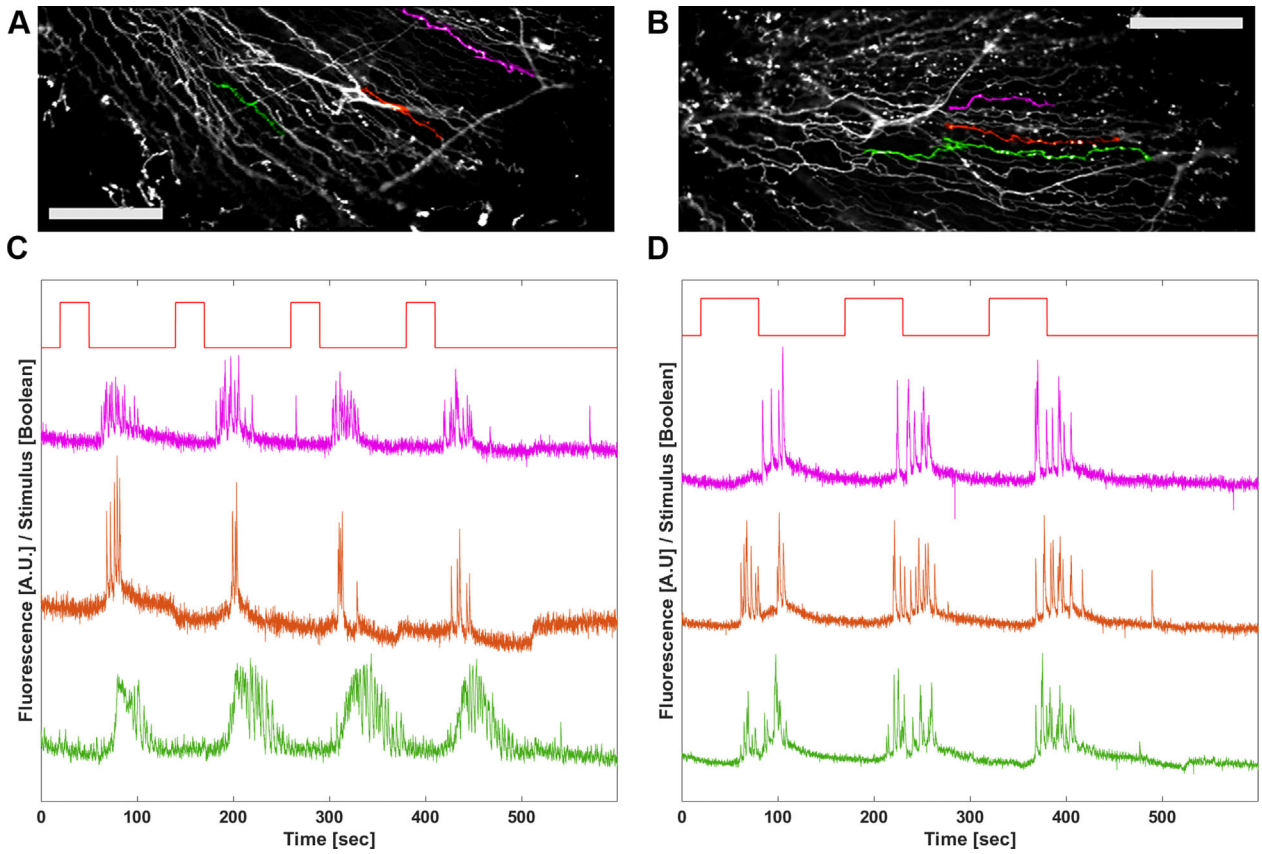

Figure 4. Average intensity projection of a region of murine cornea subjected to either 30-second (**a**) or 60-second (**b**) pulses of concentrated potassium solution with regions of interest (ROI) highlighted in various colors (magenta, orange, green). Scale bars are 100 µm. The fluorescent traces for various ROIs from (**a**), (**c**), or (**b**) and (**d**) are shown over time. ROI labels in (**a**) and (**b**) correspond with the position of the corresponding time plot in (**c**) and (**d**). Stimulus is shown at the top of the plots in red and corresponds to when the solution valve was opened at the manifold.

power at 488 nm (laser line from an argon ion laser) and a pixel residence time of approximately 0.5 µsec yielded a $\Delta F/F_0$ between 0.21 and 1.44 (SNR varying between 13 and 96) depending on the strength of the action potential (in Fig. 3b).

We applied stimulation and anesthetic to the cornea to demonstrate the feasibility of stimulus–response experiments. Concentrated potassium was added to the buffer to elicit action potentials in pulses of 30 seconds or 60 seconds, as shown in Figure 4, Supplementary Videos S2, and Supplementary S3. Stimulated action potential responses consisting of many action potentials were observed after each pulse of potassium solution. The timing of the response was consistent with and equivalent to the approximate residence time of the potassium solution on the cornea. There was a delay between each stimulus and response corresponding with the delay between the solution valve opening and the solution reaching the cornea. The number, amplitude, and timing of action potentials in each stimulus response are consistent for each repeated stimulus and suggest a consistent response for different types of nerves in the various regions of interest. Minimal photobleaching was observed across the 10 minutes measured in each experiment with an average laser power of approximately 165 µW and pixel residence time of approximately 1.0 µsec.

To test the response of the corneal nerves to an anesthetic, we applied a high dose of lidocaine (10 mM, 75 seconds) in aCSF to a cornea. Lidocaine in this concentration is expected to be neurotoxic and cause a large increase in intracellular Ca^{2+} ions followed by an anesthetic effect.[48] This phenomenon is clearly seen in Figure 5 and Supplementary Video S4, where the initial baseline signaling is followed by a large increase in intracellular Ca^{2+} (indicated by an increase in fluorescence of GCaMP6f) after the first application of lidocaine and then quiescence. A second lidocaine bolus (10 mM, 60 seconds) elicited a similar, but slightly smaller response. Last, a demonstration of alternating applications of potassium (0.3 M, 60 seconds) and lidocaine (10 mM, 60 seconds) is shown in Supplementary Figure S3. From these data, we qualitatively observe differential, but repeatable responses to lidocaine and potassium stimulus.

Discussion

This work represents significant progress toward developing tools for the functional study of the corneal nerves and assessing the response of the corneal nerves to arbitrary stimuli. Functional study using GECIs is a large improvement over previous work using calcium dyes in terms of high SNR with low light exposure and also features low photobleaching, ease of use, imaging over a large field of view and minimal perturbation to the cornea. Additionally, imaging of the corneal innervation shown in Figure 1 is comparable in quality with previous work in transgenic murine models[49]

Investigative Ophthalmology & Visual Science

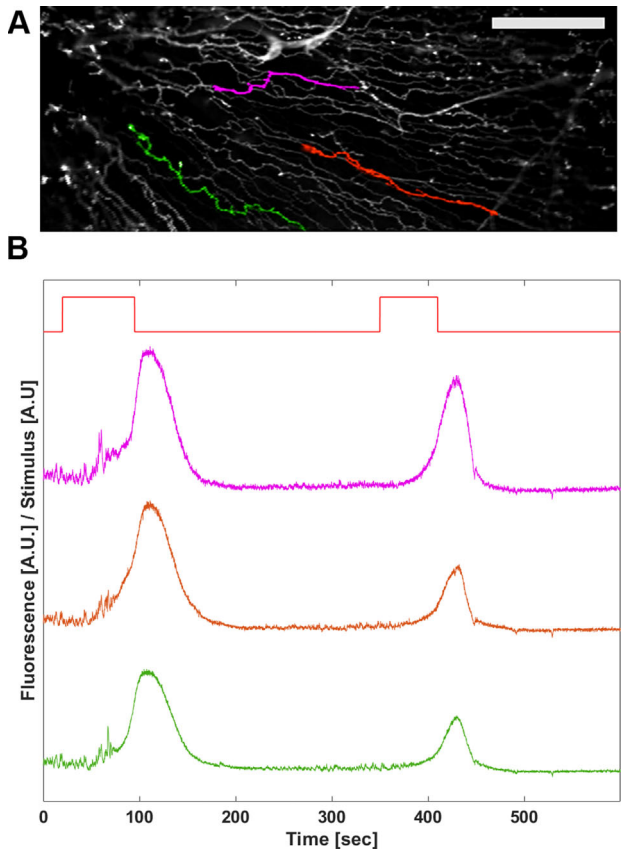

Figure 5. Average intensity projection of a region of murine cornea subjected to two pulses of concentrated lidocaine solution with regions of interest (ROI) highlighted in various colors (magenta, orange, green). The scale bar is 100 µm. The fluorescent traces for representative ROIs from (**a**) are shown over time in (**b**). ROI labels in **a** correspond to the position of the corresponding time plot in (**b**). Stimulus is shown at the top of the plots in red and corresponds with when the solution was turned on at the manifold.

and clinical imaging of humans.[29] This finding suggests that, in addition to functional imaging, this model may be used for tracking of morphologic changes to the corneal nerves. In general, the field of view demonstrated in the functional imaging is large and could potentially be extended to include the majority of the murine cornea.

We envision that this functional imaging method on ex vivo corneas could be a useful tool for assessing changes to the corneal nerves in population studies of disease and injury. To achieve this potential, further work is needed to assess the normal response of the corneal nerves to various stimuli, including chemical and mechanical stimuli. Our work here showed that various drugs, such as potassium and lidocaine, give repeatable responses to repeated stimulations and suggest that chemical stimuli might be used for assessing changes in neural responses. However, our work here also reinforces that the idea that the corneal nerve network is complicated and response to stimulus may be different for different groups and types of nerves. This result highlights the need for further study and characterization of the corneal innervation. With that characterization, this technique could be powerful for assessing the efficacy of interventions to treat corneal neuropathy in the context of neurotrophic keratopathy or diabetes. Similarly, this technique could be used to assess functional changes to the corneal nerves in response to damage caused by refractive surgery and subsequent healing.

Future work could greatly increase the potential of this technique. One major limitation of this work is that all imaging was done with the cornea in solution, limiting the ability to assess the response of the corneal nerves to fluid evaporation. In the future, this technique could be adapted to work with the imaging system in air through modification of the optics to account for the curvature of the cornea. This technique would also be a step toward in vivo imaging. Ex vivo experiments have a variety of applications, but development of a comparable method for in vivo imaging would allow for longitudinal studies of the same nerves and same animals across the progression of disease and healing over time. The speed of calcium reporters is not suitable for imaging fast neural signaling, and developing a model and imaging system using genetically encoded voltage indicators could be a significant extension to the current technique.

We feel the tools presented here have significant potential to improve the study of the corneal nerves in health and disease. The cornea is uniquely accessible for optical imaging with potentially little intervention. This work coincides with the first clinically available interventions to treat corneal nerve dysfunction and when the need for preclinical study of the impacts of interventions on various disease states is greater than ever. Better preclinical tools for assessing interventions have the potential to be revolutionary in this field. Additionally, because of the potential to view neural signaling over a large field of view with high SNR, the method could be used to decode neural circuitry, further providing a window into the effects of disease on the peripheral nerves.

Acknowledgments

The authors thank Craig Hodges, Brittany Burns, and Alma Genta for their assistance creating and maintaining the mice used in this work; Yuankai Tao for helpful consultations in the conception of this project; Yehe Liu for consultations regarding image processing; and the CWRU SOM Light Microscopy Core Facility for use of a Leica SP8 confocal microscope.

Supported by funding from the following NIH Grants: R21-EY031525, R01-HL126747, 1OT2OD025307, S10-OD024996, T32-EB007509, T32-HL134622-03, T32-EY007157, T32-EY024236, and S10-OD016164.

Disclosure: **M.T. McPheeters,** None; **B.J. Blackburn,** None; **W.J. Dupps,** None; **A.M. Rollins,** None; **M.W. Jenkins,** None

References

1. Yang AY, Chow J, Liu J. Corneal innervation and sensation: The eye and beyond. *Yale J Biol Med*. 2018;91(1):13–21.
2. Al Aqaba MA, Dhillon VK, Mohammed I, Said DG, Dua HS. Corneal nerves in health and disease. *Prog Retin Eye Res*. 2019;73:100762, doi:10.1016/j.preteyeres.2019.05.003.
3. De Cillà S, Ranno S, Carini E, et al. Corneal subbasal nerves changes in patients with diabetic retinopathy: an in vivo confocal study. *Investig Ophthalmol Vis Sci*. 2009;50(11):5155, doi:10.1167/iovs.09-3384.
4. Messmer EM, Schmid-Tannwald C, Zapp D, Kampik A. In vivo confocal microscopy of corneal small fiber damage in diabetes mellitus. *Graefes Arch Clin Exp Ophthalmol*. 2010;248(9):1307–1312, doi:10.1007/s00417-010-1396-8.
5. Rosenberg ME, Tervo TM, Immonen IJ, Müller LJ, Grönhagen-Riska C, Vesaluoma MH. Corneal structure and sensitivity in type 1 diabetes mellitus. *Invest Ophthalmol*

Vis Sci. 2000;41(10):2915–2921, https://iovs.arvojournals.org/article.aspx?articleid=2123743. Accessed June 6, 2019.

6. Midena E, Brugin E, Ghirlando A, Sommavilla M, Avogaro A. Corneal diabetic neuropathy: a confocal microscopy study. *J Refract Surg*. 2006;22(9 Suppl):S1047–S1052, doi:10.1007/s00125-003-1086-8.
7. Qu J, Li L, Tian L, Zhang X, Thomas R, Sun X-G. Epithelial changes with corneal punctate epitheliopathy in type 2 diabetes mellitus and their correlation with time to healing. *BMC Ophthalmol*. 2018;18(1):1, doi:10.1186/s12886-017-0645-6.
8. Bitirgen G, Ozkagnici A, Malik RA, Kerimoglu H. Corneal nerve fibre damage precedes diabetic retinopathy in patients with type 2 diabetes mellitus. *Diabet Med*. 2014;31(4):431–438, doi:10.1111/dme.12324.
9. Petropoulos IN, Ferdousi M, Marshall A, et al. The inferior whorl for detecting diabetic peripheral neuropathy using corneal confocal microscopy. *Invest Ophthalmol Vis Sci*. 2015;56(4):2498–2504, doi:10.1167/iovs.14-15919.
10. Mocan MC, Durukan I, Irkec M, Orhan M. Morphologic alterations of both the stromal and subbasal nerves in the corneas of patients with diabetes. *Cornea*. 2006;25(7):769–773, doi:10.1097/01.ico.0000224640.58848.54.
11. Dua HS, Said DG, Messmer EM, et al. Neurotrophic keratopathy. *Prog Retin Eye Res*. 2018;66:107–131, doi:10.1016/j.preteyeres.2018.04.003.
12. Ting DSJ, Figueiredo GS, Henein C, et al. Corneal neurotization for neurotrophic keratopathy. *Cornea*. 2018;37(5):641–646, doi:10.1097/ICO.0000000000001522.
13. Fung SSM, Catapano J, Elbaz U, Zuker RM, Borschel GH, Ali A. In vivo confocal microscopy reveals corneal reinnervation after treatment of neurotrophic keratopathy with corneal neurotization. *Cornea*. 2018;37(1):109–112, doi:10.1097/ICO.0000000000001315.
14. Mastropasqua L, Nubile M, Lanzini M, Calienno R, Dua HS. In vivo microscopic and optical coherence tomography classification of neurotrophic keratopathy. *J Cell Physiol*. 2019;234(5):6108–6115, doi:10.1002/jcp.27345.
15. Clayton JA. NEJM review: dry eye. *N Engl J Med*. 2018;378(23):2212–2223, doi:10.1056/NEJMra1407936.
16. Quinto GG, Camacho W, Behrens A. Postrefractive surgery dry eye. *Curr Opin Ophthalmol*. 2008;19(4):335–341, doi:10.1097/ICU.0b013e3283009ef8.
17. Denoyer A, Landman E, Trinh L, Faure J-F, Auclin F, Baudouin C. Dry eye disease after refractive surgery. *Ophthalmology*. 2015;122(4):669–676, doi:10.1016/j.ophtha.2014.10.004.
18. Darwish T, Brahma A, O'Donnell C, Efron N. Subbasal nerve fiber regeneration after LASIK and LASEK assessed by noncontact esthesiometry and in vivo confocal microscopy: prospective study. *J Cataract Refract Surg*. 2007;33(9):1515–1521, doi:10.1016/j.jcrs.2007.05.023.
19. Kauffmann T, Bodanowitz S, Hesse L, Kroll P. Corneal reinnervation after photorefractive keratectomy and laser *in situ* keratomileusis: an in vivo study with a confocal videomicroscope. *Ger J Ophthalmol*. 1996;5(6):508–512, http://www.ncbi.nlm.nih.gov/pubmed/9479547. Accessed June 6, 2019.
20. Darwish T, Brahma A, Efron N, O'Donnell C. Subbasal nerve regeneration after LASEK measured by confocal microscopy. *J Refract Surg*. 2007;23(7):709–715, http://www.ncbi.nlm.nih.gov/pubmed/17912941. Accessed June 6, 2019.
21. Al-Aqaba M, Calienno R, Fares U, et al. The effect of standard and transepithelial ultraviolet collagen cross-linking on human corneal nerves: an ex vivo study. *Am J Ophthalmol*. 2012;153(2):258–266.e2, doi:10.1016/j.ajo.2011.07.006.
22. Epidemiology T, Disease DE. The epidemiology of dry eye disease: report of the Epidemiology Subcommittee of the International Dry Eye WorkShop (2007). *Ocul Surf*. 2007;5(2):93–107, doi:10.1016/S1542-0124(12)70082-4.
23. Centers for Disease Control and Prevention. *National diabetes statistics report, 2020*. Washington, DC: Centers for Disease Control and Prevention; 2020.
24. McQuillan G, Kruszon-Moran D, Flagg EW, Paulose-Ram R. Prevalence of herpes simplex virus type 1 and type 2 in persons aged 14-49: United States, 2015-2016. *NCHS Data Brief*. 2018;304:1–8.
25. Mayeux R, Stern Y. Epidemiology of Alzheimer disease. *Cold Spring Harb Perspect Med*. 2012;2(8)a006239, doi:10.1101/cshperspect.a006239.
26. Zhao Y, Fu JL, Li YL, Li P, Lou FL. Epidemiology and clinical characteristics of patients with glaucoma: an analysis of hospital data between 2003 and 2012. *Indian J Ophthalmol*. 2015;63:825–831, doi:10.4103/0301-4738.171963.
27. Dana R, Bradley JL, Guerin A, et al. Estimated prevalence and incidence of dry eye disease based on coding analysis of a large, all-age United States health care system. *Am J Ophthalmol*. 2019;202:47–54, doi:10.1016/j.ajo.2019.01.026.
28. Golebiowski B, Papas E, Stapleton F. Assessing the sensory function of the ocular surface: implications of use of a non-contact air jet aesthesiometer versus the Cochet-Bonnet aesthesiometer. *Exp Eye Res*. 2011;92(5):408–413, doi:10.1016/j.exer.2011.02.016.
29. Kalteniece A, Ferdousi M, Adam S, et al. Corneal confocal microscopy is a rapid reproducible ophthalmic technique for quantifying corneal nerve abnormalities. *PLoS One*. 2017;12(8):e0183040, doi:10.1371/journal.pone.0183040.
30. Patel D V., McGhee CNJ. In vivo confocal microscopy of human corneal nerves in health, in ocular and systemic disease, and following corneal surgery: a review. *Br J Ophthalmol*. 2009;93(7):853–860, doi:10.1136/bjo.2008.150615.
31. Al-Aqaba MA, Dhillon VK, Mohammed I, Said DG, Dua HS. Corneal nerves in health and disease. *Prog Retin Eye Res*. 2019;73:100762, doi:10.1016/j.preteyeres.2019.05.003.
32. Drug Approval Package: OXERVATE (cenegermin-bkbj). Available from: https://www.accessdata.fda.gov/drugsatfda_docs/nda/2018/761094Orig1s000TOC.cfm. Accessed June 10, 2019.
33. Belmonte C, Giraldez F. Responses of cat corneal sensory receptors to mechanical and thermal stimulation. *J Physiol*. 1981;321:355–368.
34. Brock JA, Pianova S, Belmonte C. Differences between nerve terminal impulses of polymodal nociceptors and cold sensory receptors of the guinea-pig cornea. *J Physiol*. 2001;533(Pt 2):493–201.
35. Gover TD, Kao JPY, Weinreich D. Calcium signaling in single peripheral sensory nerve terminals. *J Neurosci*. 2003;23(12):4793–4797, http://www.ncbi.nlm.nih.gov/pubmed/12832498. Accessed June 13, 2019.
36. Quallo T, Vastani N, Horridge E, et al. TRPM8 is a neuronal osmosensor that regulates eye blinking in mice. *Nat Commun*. 2015;6:7150, doi:10.1038/ncomms8150.
37. Kovács I, Luna C, Quirce S, et al. Abnormal activity of corneal cold thermoreceptors underlies the unpleasant sensations in dry eye disease. *Pain*. 2016;157(2):399–417, doi:10.1097/j.pain.0000000000000455.
38. Li F, Yang W, Jiang H, et al. TRPV1 activity and substance P release are required for corneal cold nociception. *Nat Commun*. 2019;10(1):5678, doi:10.1038/s41467-019-13536-0.
39. Chen T-W, Wardill TJ, Sun Y, et al. Ultra-sensitive fluorescent proteins for imaging neuronal activity. 2013;18(4997458):295–300, https://www.ncbi.nlm.nih.gov/pmc/articles/PMC3777791/pdf/nihms489004.pdf. Accessed May 1, 2017.

Investigative Ophthalmology & Visual Science

40. Guérette D, Khan PA, Savard PE, Vincent M. Molecular evolution of type VI intermediate filament proteins. *BMC Evol Biol*. 2007;7:164, doi:10.1186/1471-2148-7-164.
41. Michalczyk K, Ziman M. Nestin structure and predicted function in cellular cytoskeletal organisation. *Histol Histopathol*. 2005;20(2):665–671, doi:10.14670/HH-20.665.
42. Müller LJ, Vrensen GFJM, Pels L, Cardozo BN, Willekens B. Architecture of human corneal nerves. *Investig Ophthalmol Vis Sci*. 1997;38(5):985–994, https://iovs.arvojournals.org/article.aspx?articleid=2161847. Accessed September 11, 2020.
43. Henriksson JT, McDermott AM, Bergmanson JPG. Dimensions and morphology of the cornea in three strains of mice. *Investig Ophthalmol Vis Sci*. 2009;50(8):3648, doi:10.1167/iovs.08-2941.
44. Schindelin J, Rueden CT, Hiner MC, Eliceiri KW. The ImageJ ecosystem: an open platform for biomedical image analysis. *Mol Reprod Dev*. 2015;82(7–8):518–529, doi:10.1002/mrd.22489.
45. Schindelin J, Arganda-Carreras I, Frise E, et al. Fiji: An open-source platform for biological-image analysis. *Nat Methods*. 2012;9(7):676–682, doi:10.1038/nmeth.2019.
46. Pnevmatikakis EA, Giovannucci A. NoRMCorre: an online algorithm for piecewise rigid motion correction of calcium imaging data. *J Neurosci Methods*. 2017;291:83–94, doi:10.1016/j.jneumeth.2017.07.031.
47. Müller LJ, Marfurt CF, Kruse F, Tervo TMT. Corneal nerves: structure, contents and function. *Exp Eye Res*. 2003;76(5):521–542, doi:10.1016/S0014-4835(03)00050-2.
48. Gold MS, Reichling DB, Hampl KF, Drasner K, Levine JD. Lidocaine toxicity in primary afferent neurons from the rat. *J Pharmacol Exp Ther*. 1998;285(2):413–421.
49. Yu CQ, Rosenblatt MI. Transgenic corneal neurofluorescence in mice: a new model for in vivo investigation of nerve structure and regeneration. *Investig Ophthalmol Vis Sci*. 2007;48(4):1535–1542, doi:10.1167/iovs.06-1192.

Supplementary Material

Supplementary Video S1. Video representation of the data shown in Figure 3, sped up to approximately 3× real time. Calcium imaging of basal signaling in the corneal nerves is shown.

Supplementary Video S2. Video representation of the data shown in Figures 4a and 4c, sped up to approximately 5× real time. Repeated 30-second chemical boluses of high potassium solution are used to stimulate the corneal nerves.

Supplementary Video S3. Video representation of the data shown in Figures 4b and 4d, sped up to approximately 5× real time. Repeated 60-second chemical boluses of high potassium solution are used to stimulate the corneal nerves.

Supplementary Video S4. Video representation of the data shown in Figure 5, sped up to approximately 5× real time. Repeated boluses of lidocaine solution are used to stimulate and then inhibit the corneal nerves.

Investigative Ophthalmology & Visual Science